

Valence band photoemission from the GaN (0001) surface

T. Strasser, C. Solterbeck, F. Starrost, and W. Schattke

Institut für Theoretische Physik und Astrophysik, Christian-Albrechts-Universität, Leibnizstr. 15,
D-24098 Kiel, Germany

submitted to Phys. Rev. B, 17.05.1999

A detailed investigation by one-step photoemission calculations of the GaN (0001)-(1x1) surface in comparison with recent experiments is presented in order to clarify its structural properties and electronic structure. The discussion of normal and σ -normal spectra reveals through the identified surface states clear fingerprints for the applicability of a surface model proposed by Smith et al. [5]. Especially the predicted metallic bonds are confirmed. In the context of direct transitions the calculated spectra allow to determine the valence band width and to argue in favor of one of two theoretical bulk band structures. Furthermore a commonly used experimental method to fix the valence band maximum is critically tested.

79.60.-i, 73.20.At, 73.61.Ey

I. INTRODUCTION

The wide band gap semiconductor GaN has experienced exciting applications in blue light emitting diodes and laser diodes. For a further improvement of the quality of the material a better understanding of the structural and electronic properties is necessary. The energetic positions of critical points differ by 0.8 eV for the existing band structure calculations of wurtzite GaN [1,3]. Furthermore, the geometrical structure of the GaN (0001) surface is still being debated [4,6].

The most powerful tool for examining the electronic structure of semiconductors is the angle resolved ultraviolet photoemission spectroscopy (ARUPS). The spectra give insight into the valence band structure of the bulk as well as the surface. Besides the part of direct interest, i.e. the initial bound state, the photoemission process also involves the excitation to outgoing scattering states with the transition probability given by matrix elements. Therefore, as already demonstrated for the cubic GaN (001) surface [7], a full account of the experimental data can only be attained by a comparison with photocurrents calculated within the one-step model.

As a starting point we use a GaN (0001)-(1x1) $\sqrt{3}\sqrt{3}$ surface, as it is predicted by total energy calculations performed within the local density formalism [5]. The calculated photoemission spectra in normal emission are examined with respect to contributions from the bulk band structure as well as from surface states. For example, we identify a structure near the lower valence band edge as resulting from a surface state. Only by taking this state into account, the correct energetic position of the band

edge can be extracted. Based on the detailed understanding of the photocurrent the flexibility of the calculation allows us to adjust the underlying bulk band structure to the experimental results. This means that we are able to correct the position of the valence band maximum, which is an important value for determining band offsets and band bending. Though abandoning parameter-free modeling thereby, one gains experience how peaks are shifted and intensities are deformed by the matrix elements. The true position of the bands can be much better determined in such an interpretation of experiment than using standard band mapping methods.

σ -normal photoemission spectra provide an enhanced surface sensitivity. Near the upper valence band edge, experiment has pointed out an sp_z orbital related surface state [8]. Identifying this state, which depends sensitively on the surface geometry, in the theoretical spectra, we can connect the geometric and electronic structure with the measured photocurrents.

This paper is organized as follows. First a short overview about the theory is given, followed by a detailed analysis of the initial surface band structure and the used normal bands. Then the results for normal emission spectroscopy from the GaN (0001)-(1x1) $\sqrt{3}\sqrt{3}$ surface are presented, together with a detailed interpretation in comparison with experiment. It is shown how the theoretical band structure calculation can be related to experiment and how uncertainties in the experimental interpretation can be removed. Finally, we present the results for σ -normal emission, comparing with experimental data, too.

II. THEORY

In this section, we briefly discuss the theoretical techniques used in our calculation of the photocurrent. For details see the references [9,10].

We calculate the photocurrent within the one-step model. The photocurrent I is given by:

$$I = \sum_{i,j} \text{Im} \left[\langle \psi_i | \hat{h}_{\text{LEED}}(E_{\text{fin}}; \mathbf{k}_k) | \psi_j \rangle \langle \psi_j | \hat{h}_{\text{LEED}}(E_{\text{fin}}; \mathbf{k}_k) | \psi_i \rangle \right] \quad (1)$$

For simplicity the vector potential \mathbf{A}_0 is kept constant. $G_{i,j}$ represents the halfspace Green's function of the valence states, given in a layer-resolved LCAO basis ψ_i . Our basis set consists of the 4s and 4p atomic orbitals

of gallium and the 2s and 2p atomic orbitals of nitrogen, taking into account the coupling up to fourth nearest neighbor atoms. The Hamiltonian matrix is calculated according to the Extended-Huckel-Theory (EHT). Its parameters, employed for bulk and halfspace calculations, are adjusted to published ab-initio bulk band structures using a genetic algorithm [11]. We use two different sets for the parameters. One set is adjusted to the GW quasiparticle band structure of Rubio et al. [1]. The other set is adjusted to a self-interaction and relaxation corrected pseudopotential band structure calculation by Vogel et al. [2]. The two sets of parameters belonging to these band structures are presented in Table I. Figure 1 shows the resulting bulk band structure according to Vogel et al. (solid lines). A long \bar{A} , also the band structure adjusted to Rubio et al. is shown (dashed lines). The main difference is the energetic position of the lower valence band edge at $\bar{\Gamma}$ near -8.0 eV, where the calculations differ by nearly 0.8 eV.

The electronic structure of the surface is determined by the calculation of the k_x -resolved density of states (DOS) from the halfspace Green's matrix G_{ij} , the same as used for the photocurrent. It takes into account relaxation and reconstruction at the surface. The resolution of the DOS with respect to atomic layers and orbital composition allows for a detailed characterization of the bands and their corresponding photocurrents.

The final state of photoemission is a scattering state with asymptotic boundary conditions. For a clean surface its wave function is determined by matching the solution of the complex bulk band structure to the vacuum solution, representing the surface by a step potential [12,13]. This treatment is best suited for discussing the photoemission peaks in terms of direct transitions with conservation of the surface perpendicular wave vector k_z , since the final state is described inside the crystal as a sum over bulk solution of different k_z . These solutions of the complex bulk bands are calculated with an empirical pseudopotential. For GaN we use the pseudopotential form factors of Bloom et al. [14]. The damping of the wave function inside the crystal is described by the imaginary part of an optical potential.

In Eq. (1), the transition matrix elements $h_{LEED}(E_{fin}; k_x) \propto \sum_{ij} p_{ji}$ between the final state and layer Bloch sums are numerically integrated in real space. Their dependence on atomic layers and orbitals permits a detailed analysis of the spectra.

III. RESULTS AND DISCUSSION

A. Electronic structure

In this section we discuss our results for the electronic structure of the GaN (0001) surface. We use a surface geometry of Smith et al. [5] (shown in Fig. 2), derived from

totalenergy calculation and STM examinations. Directly atop the nitrogen atoms sits a full monolayer of gallium adatoms, forming a (1x1) surface. In Fig. 3 the surface band structure is presented, calculated with the parameters of set A in Table I. The bands are determined from the peaks in the k_x resolved DOS of the four topmost atomic layers.

Within the fundamental gap there are two surface states, labeled (a) and (b). They can be identified as p_x and p_y derived bridge bonds between the Ga adlayer atoms. Smith et al. found these strongly dispersive metallic bonds to be responsible for the stability of this surface [5]. The state (c) is built up by the Ga s and p_z orbitals, in \bar{K} and \bar{M} with strong contributions from the underlying N p_z orbitals. A long \bar{M} and mostly along \bar{K} the state (c) is in resonance with the bulk, mixing with the nitrogen p_x and p_y orbitals. Especially in $\bar{\Gamma}$, these orbitals exhibit a strong contribution to the density of states, as can be seen in Fig. 4.

A long \bar{M} the surface resonances (e) and (f) are made up by the nitrogen p_x orbitals with small contributions from the underlying Ga s and p_x orbitals. For band (d) we find strong contributions from the nitrogen p_y orbitals and from the p_y orbitals of Ga lying below the nitrogen layer. A long \bar{K} we find similar resonances (h, i, k), which can be resolved into contributions from the N p_y orbitals with a smaller amount from the N p_x and the subsurface Ga p_x and p_y orbitals. The band (g), seen at -4.0 eV near $\bar{\Gamma}$ is a nearly invisible structure in the density of states (Fig. 4), built up by broad contributions from nitrogen and gallium p_z orbitals. In the heteropolar gap we find a strong Ga s surface state (l) (see also Fig. 4) located at -8.0 eV clearly below the lower bulk band edge. As can be seen in the DOS, this state contains also contributions from the N p_z orbitals. A long \bar{M} and \bar{K} this band shows a strong dispersion towards lower binding energy, becoming a surface resonance between \bar{M} and \bar{K} . Near the lower valence band edge we find a second resonance (m) formed by the N p_x orbitals and Ga s orbitals from deeper atomic layers. In \bar{K} we find also contributions from the N p_y orbitals. Altogether, taking into account the states inside the fundamental gap and the surface state in the heteropolar gap, the surface band structure of the GaN (0001)-(1x1) Ga surface shows a similar behavior as the cubic GaN (001)-(1x1) Ga surface [15,7].

The complex final bands are shown in Fig. 5. They are calculated along the symmetry line $\bar{\Gamma}$, which corresponds to normal emission. Since we introduced an imaginary optical potential all bands are damped. The horizontal bars denote the weight which single complex bands carry in the final state. With respect to this criterion, only the four most important bands for the photoemission are shown. They have strong contributions to the final state (labeled (a), (b), (c), and (d)). Below 15 eV final state energy state (d) is the most important one. In this energy

range state (a) and (c) reveal large imaginary parts, being responsible for a strong damping of these states inside the crystal. Between 15 and 65 eV state (a) contributes dominantly. Above 65 eV band (b) yields the essential contribution to the valence state.

B. Normal Emission

Figure 6 presents normal emission spectra for the GaN (0001)-(1x1) Ga surface, which are calculated for photon energies from 14 up to 78 eV. The radiation is chosen to be incident within the xz plane at an angle of 45° to the surface normal. The radiation is polarized parallel to the plane of incidence. The spectra are dominated by two structures, near -1.0 (A) and -8.0 eV (E). The last one coincides with the strong Ga s surface state near -8.0 eV, which can be seen in the DOS at $\bar{\Gamma}$ in Fig. 4. The emission from this peak is localized in the topmost gallium layer, which can be proven by analyzing the orbital and layer resolved matrix elements, as presented in Fig. 7. For valence state energies between 8 and 21 eV the s orbitals of the gallium adlayer atoms show large matrix elements. This agrees with the strong emissions at -8 eV for photon energies between 16 and 29 eV. For higher valence state energies the Ga s matrix elements as well as the peak heights are much smaller. At 25 eV and above 40 eV valence state energy the matrix elements of the first nitrogen p_z orbitals become appreciable. So the emissions near 33, 49 eV and 78 eV photon energy are enhanced by emissions from nitrogen p_z -orbitals, although they show much weaker DOS at $\bar{\Gamma}$ near -8.0 eV than the gallium s orbitals.

The leading peak near -1.0 eV valence energy (A) is connected to the high and broad density of states (Fig. 4), resulting from the nitrogen p_x - and p_y orbitals. While emissions from the p_y orbitals are forbidden by selection rules, the nitrogen p_x matrix elements exhibit minima near 25, 50 and 73 eV valence energy. This is consistent with the decreasing intensity of the leading peak near 27, 51 and 74 eV photon energy whereby the behavior at 27 eV is especially convincing. For 51 eV the smaller intensity of the leading peak is one reason for the more pronounced intensity of those at higher binding energies, because in Fig. 6 each spectrum is normalized separately to an equal amount in the highest peak. Furthermore, for analyzing structure (A) we have to take into account direct transitions assuming exact conservation of the perpendicular wave vector. For a given excitation energy we determine the binding energies at which transitions from the initial bulk band structure into the complex valence band structure are possible. These binding energies are plotted in the photoemission spectra with bars whose length indicates the contributions of the complex band to the valence state. For structure A we have to consider the initial bands 1, 2 and 3 (see Fig. 1). Hints

for the contribution of direct transitions to structure (A) are the dispersion for photon energies between 14 and 20 eV at the lower binding energy side (from initial state (2) into valence band (d)) and between 20 and 47 eV photon energy where the leading peak disperses from -0.1 eV to -1.1 eV (initial band (1) and (2) into valence band (a)). For photon energies of 17 eV (valence band (d)), 39 eV (valence band (a)) and 74 eV (valence band (b)) shoulders from direct transitions from the VBM can be seen.

Besides the two prominent structures there exist weaker intensities with strong dispersion. (C) and (D) can be identified as emissions from the initial bands (3) and (4) into the valence bands (d) and (c), respectively. Between 28 and 63 eV photon energy we find the dispersive structure (B). It can be explained by direct transitions from the valence band (4) into the valence band (a). At 47 eV photon energy the structure reaches the highest binding energy with -7.2 eV. Near the lower valence band edge above (E) and interfering with (B) there are further weak structures in the photon range from 39 to 59 eV which result from nitrogen p_z orbitals. Near -5.5 eV emissions from the nitrogen p_z orbitals from the second nitrogen layer arise for photon energies between 49 and 59 eV. Emissions from the third nitrogen layer p_z , located at -6.7 and -3.2 eV are visible in the photon range (51, 55) eV and (39, 49) eV respectively.

Compared with the GaN (001) surface [7], direct transitions are less significant for wurtzite GaN in the range up to 78 eV photon energy. Further calculation shows, that above 98 eV photon energy a strong dispersive structure belonging to the initial state band (4) and the valence state (b) appears, reaching its highest binding energy near 118 eV photon energy.

C. Normal emission - comparison with experiment

In this section we compare our calculated spectra with experimental results in normal emission performed by Dhesiet al. [8] for photon energies between 31 and 78 eV. The measurements were done at a wurtzite GaN film, grown by electron cyclotron resonance assisted molecular beam epitaxy on sapphire substrates with subsequent annealing. The spectra were detected with synchrotron radiation, incident at 45° to the surface normal.

Figure 8 shows on the right hand side the experimental results. Energy zero is the VBM, which was determined from the spectra by extrapolating the leading edge. In comparing the spectra we will show that this technique places the experimental VBM 1.0 eV above the VBM as taken from the band structure.

On the left hand side of Fig. 8 our theoretical results, as discussed in the section (B), are plotted (solid lines). The experimental data show a dominant structure near -2.0 eV which can be associated with the theoretical

peak at -1.0 eV. Like the theoretical results, this structure exhibits some dispersion to lower binding energies between 63 and 66 eV photon energy (theory between 59 and 63 eV). These emissions can be explained by transitions from the $N p_x$ orbitals and by direct transitions from the bulk bands (1) and (2). Furthermore, the experimental results reveal a dispersing structure between -4.2 and -8.2 eV, which is also visible in the theoretical results (between -3.2 and -7.2 eV). In both series, the emissions from that structure become weak for photon energies around 39 eV. Near 55 eV photon energy both experiment and theory show enhanced emissions, dispersing back to lower binding energies. A round 66 eV photon energy the emissions near -4.0 eV are much weaker in theory than in experiment. The theoretical spectra show a significant doubling of the leading peak at $h\nu = 78$ eV, with emissions near -0.8 eV and -1.8 eV. A similar effect is not seen in the experimental results of Dhesi et al. However, recent measurements by Ding et al. display the double maximum [16]. The latter experiment was performed on a GaN (0001)-(1x1) surface, also grown on sapphire but by means of metalorganic chemical vapour deposition (MOCVD). For photon energies of 75 and 80 eV the experimental spectra by Ding et al. show peaks near the upper valence band edge and near -2.0 eV, which can be connected to the peaks in the theoretical spectra for 74 and 78 eV photon energy.

All over all, we can identify two significant structures from the experimental data by Dhesi et al. in our calculated spectra. Comparing their energetical position we recognize, that the theoretical structures are at 1.0 eV lower binding energy. We explain this difference by an inaccuracy of the experimentally determined VBM of 1.0 eV. It should be pointed out, that this error also explains the energetical shift of 1.0 eV which is necessary to match the experimental band structure of Dhesi et al. with the theoretical band structure in Ref. [8].

Apart from the two discussed series, Fig. 8 includes some dashed lined theoretical spectra. These spectra are calculated with the EHT parameters of set B, see Table I. The parameters are related to the band structure of Rubio et al. with a valence band width of 8.0 eV. The spectra are similar to the calculated results already discussed. The leading peak is almost unchanged, while the emissions near the lower valence band edge are shifted by 0.8 eV. This statement is true for the whole theoretical series calculated with the parameters of set B. Comparing with experiment, we can point out two results. The leading peak between -1.0 and -0.3 eV in both theoretical series can be identified with the experimental structure between -2.0 and -1.2 eV. This underlines that the experimental VBM has to be shifted by nearly 1.0 eV to higher binding energies as already stated. Similarly the emissions near -8.2 eV in the experimental spectra can be assumed to lie at -7.2 eV, which would be consistent with the theoretical spectra calculated by the band structure

of Vogel et al. [2] (parameters of set A). This means that we are able to determine the valence band width to 7.2 eV, by comparing the experimental spectra with calculated photocurrents based on different band structures.

Furthermore, in the experimental paper of Dhesi et al. it is pointed out that at lower photon energies a non-dispersive feature with a binding energy of approximately -8.0 eV is visible [8]. In Ref. [8] the peak is explained with a surface state or density of state effects, rather than with a surface state. Our examination however, for photon energies lower than 30 eV clearly reveals significant emissions from a gallium s surface state at that energy, and not from the band edge (see section (B)). The theoretical band edge is found at 0.8 eV lower binding energy, and additionally, the variation of the intensity with photon energy is associated with the matrix elements and uniquely attributes this emission to a surface state. In both the theoretical and experimental spectra weak emissions for photon energies between 31 and 39 eV around the lower valence band edge are observed which can be additionally attributed to the surface band emission (see Fig. 8). Near -8.0 eV the experiment shows enhanced emissions for photon energies between 47 and 55 eV, which are also seen in the theory around -7.2 eV. The experimental peaks at highest binding energy are broad enough for including also the emissions from the surface state near -8.0 eV in theory (gallium s and nitrogen p_z related). The association of a non-dispersive structure with a theoretically estimated band edge merely because of its energetical vicinity can easily lead to erroneous band mapping [7], especially as surface states often develop near band edges.

Summarizing the above discussion, we have demonstrated that there is a clear agreement between the theoretical and experimental results for a wide energy range. This agreement allows us to show that the determination of the VBM by extrapolating the leading edge could involve significant errors. The determination of the VBM is an important step in the investigation of band bending and valence band discontinuity in heterojunctions [17,18]. Especially, Wu et al. [18] investigated the band bending and the work function of wurtzite GaN (0001)-(1x1) surfaces by ultraviolet photoemission. By extrapolating the leading peak, the VBM was determined at 2.4 eV above the strong structures, which are located in our theory around -1.0 eV. The difference in the positions of the VBM is 1.4 eV being much more than the accuracy of 0.05 eV which is assumed for this technique [17]. The error in the experimental VBM determination by extrapolation appears to be critical. Beside the VBM the detailed comparison of calculated and measured photocurrents allows us to determine the bulk band width to 7.2 eV. Furthermore we identify emissions from a surface state, which is related to the gallium adlayer. These emissions are a first hint for the reliability of the used surface geometry and will be further analyzed with the

more surface sensitive σ -normal photoemission in the next section.

D. σ -normal emission - theory

Priority of section (B) and (C) was given to analyze the electronic bulk features from σ -normal emission spectroscopy. In this section we present theoretical results for σ -normal emission along the \bar{M} and the \bar{K} direction. In addition to the electronic structure we are now interested in the geometric structure of the surface. In this context it seems necessary to examine the real space origin of the photocurrent, which is done for two examples before we consider the whole series.

Figure 9 shows two layer resolved spectra in the \bar{M} direction. They are calculated for emission angles of 0° (normal emission) and 18° with photon energies of 50 and 55 eV respectively. The numbers at the layer resolved spectra indicate the number of layers which have been used in the sum of Eq. 1, starting with the topmost layer. The spectra are shown together with the density of states, the bulk valence bands, and the complex valence bands. The DOS is calculated for different k_x , referring to the plotted angles and binding energies, such that they can directly be compared with the photocurrents. Also the bulk bands are calculated taking into account the correct k_x . The complex valence bands are shifted by the excitation energy onto the valence band structure. For the photoemission spectra the light impinges in the yz plane with a polar angle of 45° .

For normal emission six peaks can be seen in the photocurrent (Fig. 9). The double peak (C) can be explained by direct transitions from the two topmost valence bands. The positions of the direct transitions are indicated by the dashed lines. As the peak at the lower binding energy side becomes visible above the third layer (12 atomic planes), the peak at the higher binding energy side shows also contributions from the surface layer. These contributions are related to emissions from the nitrogen p_z and p_y orbitals which yield the largest matrix elements. Peak (H) is only a weak structure. It is explained by direct transitions into valence bands which contribute less to the outgoing state. (G) and (G') are direct transitions from the lower valence bands into the two major valence bands. Especially for (G) also emissions from the nitrogen p_z orbitals from the third and fourth nitrogen layer have to be taken into account. Peak (I) is clearly related to the emissions from the gallium s and nitrogen p_z surface state located in the first atomic layers, as already explained in the section (B).

Changing the emission angle to 18° two emissions (A) and (B) appear, which are due to the surface states (a) and (c) respectively (see Fig. 3). Both structures have their origin in the first atomic layers. The structures

(C) and (D) are explained by direct transitions. In contrast to the structure (C), which is visible above the third layer, structure (D) shows an enhanced contribution from the surface layer (nitrogen p_y and p_z). These contributions are larger than those for the double peak (C) in normal emission at -1.0 eV. The remaining peaks can be explained by direct transitions with weak contributions from the nitrogen p_z and p_x orbitals of the surface layers.

Summarizing, we found an enhanced surface sensitivity for higher angles. This regards the states within the gap, as well as resonant structures (e.g. (D) in Fig. 9). The enhanced surface sensitivity at σ -normal angles is well known and has been recently investigated by one-step model calculations [19].

In Fig. 10 a series along the \bar{M} direction is presented. The structure (A) can be related to the surface state (a) in the surface band structure (see Fig. 3) and is built up by emissions from the topmost nitrogen p_z and gallium p_z and p_x orbitals. The emissions from structure (B) are related to the same orbitals and belong to the surface state (c). The structure (C) can be found at all angles. A part from direct transitions also emissions from the nitrogen p_z and p_y orbitals contribute. Especially, the structure (D) displays besides direct transitions the DOS of the first 8 atomic layers (see Fig. 9). The emissions (E) and (F) can be explained by the surface resonances (e) and (f) (see Fig. 3) which frame a gap in the projected bulk band structure. The emissions are related to nitrogen p_x orbitals of the first three layers with varying contributions from direct transitions. The dispersion of structure (G) follows the lower valence band edge, and in addition to direct transitions, emissions from nitrogen p_x and p_z orbitals are responsible for this structure. Structure (I) belongs to the surface state (l), see Fig. 3. The structure (G') is connected to direct transitions as can be seen in Fig. 9.

In Fig. 11 the theoretical photocurrents along the \bar{K} direction are shown. The spectra are calculated for angles between 0° and 30° , with photon energies between 50 and 66 eV. The light is p -polarized and incident along the xz -plane with an angle of 45° with respect to the surface normal. Because of the high emission angles also the \bar{K} direction is reached.

The theoretical spectra show a weak emission (A) for angles around 18° . This emission represents the surface band (a) between $\bar{\Gamma}$ and \bar{K} , which can be seen in Fig. 3. Structure (B) results from the surface band (c), which leaves at 14° the projected bulk band structure. The structures (C) and (C') can be explained by direct transitions from the topmost valence bulk band. Additionally emission from the huge density of states from the N p_x orbitals have to be taken into account (see the discussion of Fig. 9). The emission (D) results from nitrogen p_z orbitals below the first layer. For angles below 14° the structure (E) stems from the surface resonance (k) (see Fig. 3). It consists of nitrogen p_y orbitals and shows

large dispersion to higher binding energies. Above 14 (E) interferes with emissions from the surface resonance (I). The structure (F) belongs to the surface resonance (I) consisting of nitrogen p_z and gallium s orbitals, with the main contributions from the nitrogen surface atoms. The remaining structures (H, G, G' and I) are explained as their counterparts for the \bar{M} direction.

In both theoretical spectra we are able to identify emissions which are related to the orbital composition of the topmost surface layers. Moreover, also emissions from resonances show contributions from the surface, as has been pointed out by the layer resolved photocurrent. If we are able to identify these emissions in experimental data, clear fingerprints for the assumed gallium adlayer structure would be indicated.

E.0 \bar{O} -normal emission - comparison with experiment

In this section we compare our results in \bar{O} -normal emission with experimental data of Dhesi et al. [8]. For comparing the spectra, it is also important here to take into account the shift of 1.0 eV, which is necessary to adjust the VBM (see section C).

In Fig. 10 the spectra for \bar{M} are shown. At low binding energies the experiment shows strong emissions, which are identified with the structure (C) in the theoretical spectra. Near -8.0 eV the experiment shows a structure, which disperses to lower binding energy for higher angles with decreasing intensity. This behavior is also seen in the theoretical structure (G). The energetic difference between the two experimental structures coincides in \bar{M} with the theoretical valence band width of 7.2 eV and underlines the results from section C.

For angles above 14 the experimental data display a shoulder between -1.0 and -2.0 eV. This emission can be associated with structure (B) in theory. For 16 and 18 the shoulder becomes very broad, which may be attributed to the theoretical emissions (B) and (A). The theoretical orbital composition of these states is consistent with the results of Dhesi et al., who examined the dependence of this shoulder on polarization and contamination. The theoretical spectra show a further emission from a surface state (I). This emission might be identified with the high binding energy shoulder in the experimental data near -9.0 eV. Around -4.0 eV, the experiment shows two dispersing structures. These structures can be connected with the theoretical emissions (E) and (F) which appear to be weaker, however. Also the structure (G') is seen in experiment as a weak shoulder at low emission angles. Between -4.0 and -5.0 eV the experiment shows a structure ($\theta = 0 \dots 8$) not being marked which is related to the theoretical structure (H). Thus three surface states and several surface resonances can

be identified in experiment. Taking into account the influence of the topmost atomic layers to the photocurrent (see section D) the coincidence of the theoretical and experimental spectra confirm the used surface geometry. Moreover, considering the energetic shift of 1.0 eV, the energetic positions of the structures confirm the used surface band structure.

Further information can be reached with the results along the \bar{K} direction (Fig. 11). For angles above 14 experimental data show a structure near -1 eV. This structure can be associated with the emission (B) in the theoretical curves which results from the nitrogen and gallium surface state. Compared to experiment theory heavily overestimates the intensity. Also, the theoretical band takes off from the projected band structure background with rather strong dispersion already at 18 (see also (c) in Fig. 3) delayed by 4 with respect to experiment, where this band clearly appears already at 14 with very low dispersion. This difference is a hint that the theoretical surface band (c) becomes free of the projected bulk band structure with smaller dispersion along \bar{K} and significant closer to the $\bar{\Gamma}$ point than obtained in our surface band structure calculation. In the same energy range but for lower angles, a shoulder is marked in the spectra which is comparable with the structure (C') in theory.

Near -2.0 eV experiment marks a structure, dispersing a little to higher binding energy for larger angles. This structure can be identified with the theoretical emission (C), visible for angles between 0 and 12. The experimental structure disperses from -2.0 eV to -3.0 eV, while the theoretical structure disperses from -0.9 eV to -2.4 eV at 12. Above 14 the experiment shows no peaks for this structure, but only shoulders. The theoretical curves show the structures (D) and (E), which explains for higher angles these shoulders and the adjacent experimental peaks on the higher binding energy side.

Below 14 structure (E) reproduces the dispersive experimental structure between -2.6 and -5.6 eV. Different from experimental data, the emission (E) is less pronounced and displays less dispersion (about 300 meV). At still lower angles a weak emission (H) is seen, which is visible as a weak structure in the experimental data. Near the lower valence band edge, theory shows three structures (G, G' and I) which can be compared with the experimental structure around -8 eV. It displays similar behavior as the theoretical data with respect to dispersion and magnitude, though the experimental emissions are weaker.

Summarizing, we are able to explain all observed experimental structures. The observed energetical positions underline our result in normal emission, namely that the band width is 7.2 eV and that the experimental valence band maximum has to be shifted for 1.0 eV to higher binding energies. In addition to direct transitions all emissions in \bar{O} -normal emission are influenced

by surface states and resonances, as has been verified by the layer resolved photocurrent. This demonstrates the surface sensitivity of the experiment, misleading the mapping of valence bulk bands solely from normal measurements [8]. Also, we are able to identify three surface emissions, which show the same energetical and intensity behaviour in theory and experiment. They can be related to emissions from the topmost nitrogen p_z and gallium s and p_x orbitals. The theoretical dispersion is only slightly at variance with experiment. The emissions from the topmost atomic layers sensitively depend on surface structure and reconstruction. Thus the comparison between experimental and theoretical results confirms the reliability of the assumed theoretical surface model.

IV. CONCLUSION

Photoemission spectra in normal and σ -normal emission for the GaN (0001)-(1x1)G surface have been calculated within the one-step model. Normal emission spectra show emissions from a surface state near the lower valence band edge. It is identified by its energetic position different from the band edge and its varying intensity by inspection of the matrix elements. Furthermore, we demonstrate that a widespread experimental method to determine the VBM by extrapolating the leading edge of the valence band spectra may fail by as much as 1.0 eV. Taking this into account all the experimental structures can be identified in close agreement with theory. Especially, the valence band width (7.2 eV) agrees with a LDA bulk band structure calculation of Vogel et al. whereas a GW calculation of Rubio et al. differs by 0.8 eV.

In σ -normal emission, surface states near the upper valence band edge can be identified and analyzed with respect to surface band structures. Several surface resonances are examined and verified by experimental data. Agreement of surface specific properties in the theoretical and experimental photocurrents is seen as a proof of the used surface geometry. The surface is nitrogen terminated with a gallium adlayer.

The experimental emissions are traced back by theory to their origin in band structure, electronic states, orbital composition and location in direct space. Thus the one-step model calculation is a powerful tool to yield essential insight into the bulk and surface electronic structure. In addition, it gives credit to the underlying surface geometry. This work stresses the necessity of such a calculation for a reliable interpretation of experimental ultraviolet photoemission data in comparison with calculated band structures.

V. ACKNOWLEDGMENTS

Discussions with Prof. M. Skibowski and Dr. L. Kipp are gratefully acknowledged. We thank Prof. K. E. Smith providing us the experimental figures. The work was supported by the BM BF, under contract no. 05 SB 8 FKA 7.

-
- [1] A. Rubio, J. L. Corkill, M. L. Cohen, E. L. Shirley, and S. G. Louie, Phys. Rev. B 48, 11810 (1993).
 - [2] D. Vogel, P. Kugler, and J. Pollmann, Phys. Rev. B 55, 12836 (1996).
 - [3] Y. C. Yeo, T. C. Chong, and M. F. Li, J. Appl. Phys. 83, 1429 (1998).
 - [4] K. Rapcewicz, M. B. Nardelli, and J. Bemholc, Phys. Rev. B 56, R12725 (1997).
 - [5] A. R. Smith, R. M. Feenstra, D. W. Greve, J. Neugebauer, and J. E. Northrup, Phys. Rev. Lett. 79, 3934 (1997).
 - [6] J. Fritsch, O. F. Sankey, K. E. Schmidt, and J. B. Page, Phys. Rev. B 57, 15360 (1998).
 - [7] T. Strasser, F. Starrost, C. Solterbeck, and W. Schattke, Phys. Rev. B 56, 13326 (1997).
 - [8] S. S. Dhesi, C. B. Stagarescu, K. E. Smith, D. Doppalapudi, F. Singh, and T. D. Moustakas, Phys. Rev. B 56, 10271 (1997).
 - [9] J. Henk, W. Schattke, H.-P. Bamscheidt, C. Janowitz, R. Manzke, and M. Skibowski, Phys. Rev. B 39, 13286 (1989).
 - [10] J. Henk, W. Schattke, H. Carstensen, R. Manzke, and M. Skibowski, Phys. Rev. B 47, 2251 (1993).
 - [11] F. Starrost, S. Bomholdt, C. Solterbeck, and W. Schattke, Phys. Rev. B 53, 12549 (1996); 54, 17226 (1996).
 - [12] H. Bross, Surf. Sci. 213, 215 (1989).
 - [13] J. B. Pendry, J. Phys. C 2, 2273 (1969).
 - [14] S. Boom, G. Harbeke, E. Meier, and I. B. Ortenburger, phys. stat. sol. (b) 66, 161 (1974).
 - [15] J. Neugebauer, T. Zywietz, M. Scheer, J. E. Northrup, and C. G. Van der Walle, Phys. Rev. Lett. 80, 3097 (1998).
 - [16] S. A. Ding, S. R. Bamann, K. Hom, and V. L. Aker-

ovich, Proceedings of the 23rd International Conference on the Physics of Semiconductors, edited by M. Scheer and R. Zimmernann (World Scientific, Singapore, 1996), p. 525.

- [17] S. A. Ding, S. R. Bamann, K. Hom, H. Yang, B. Yang, O. Brandt, and K. Plog, *Appl. Phys. Lett.* 70, 2407 (1997).
- [18] C. I. Wu, A. Kahn, N. Taskar, D. Domnan, and D. Gallagher, *J. Appl. Phys.* 83, 4249 (1998).
- [19] C. Solterbeck, O. Tiedje, F. Starrost, and W. Schattke, *J. Electron Spectrosc. Relat. Phenom.* 88-91, 563 (1998).

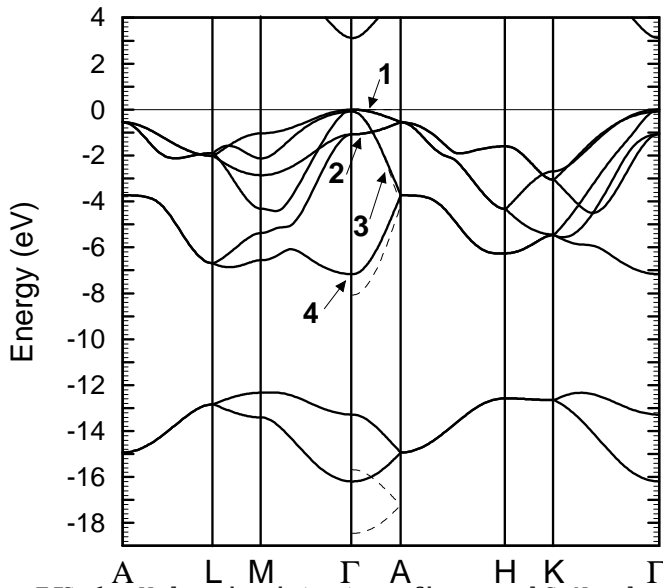


FIG. 1. Valence band structure of hexagonal GaN calculated with EHT-parameters according to Table I (solid line: set A, dashed line: set B).

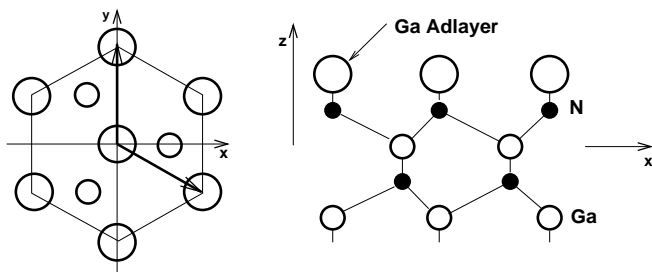


FIG. 2. The geometry of the GaN (0001)-(1x1) Ga surface according to [5].

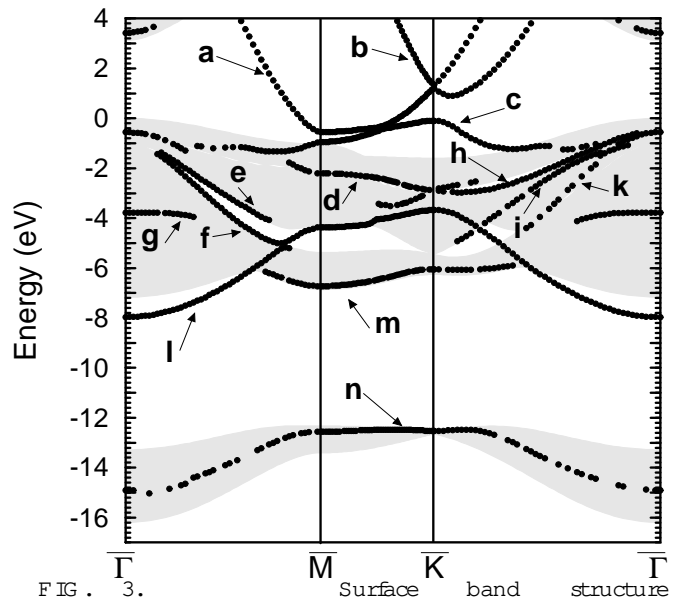


FIG. 3. Surface band structure of the GaN (0001)-(1x1) Ga surface and the projected GaN bulk band structure (shaded). For the calculation parameter set A according to Vogel et al. [2] was used.

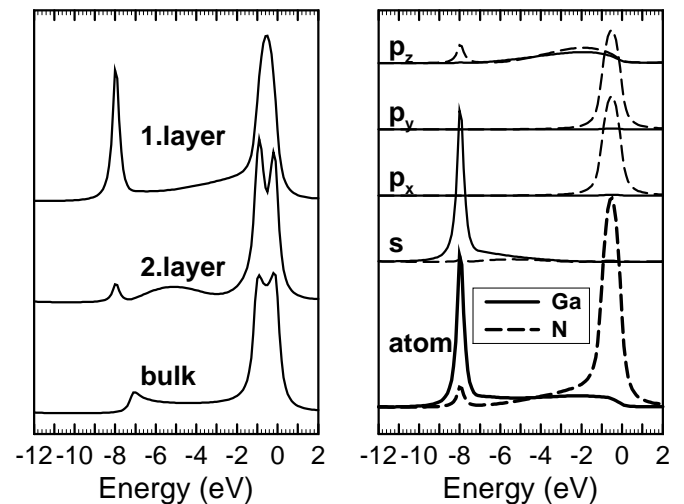


FIG. 4. Density of states at $\bar{\Gamma}$ for GaN (0001)-(1x1) Ga. On the left hand side the layer resolved DOS is shown, while on the right the DOS of the first layer is further resolved into its atomic and orbital contributions. Calculated with the parameters from set A (see Table I).

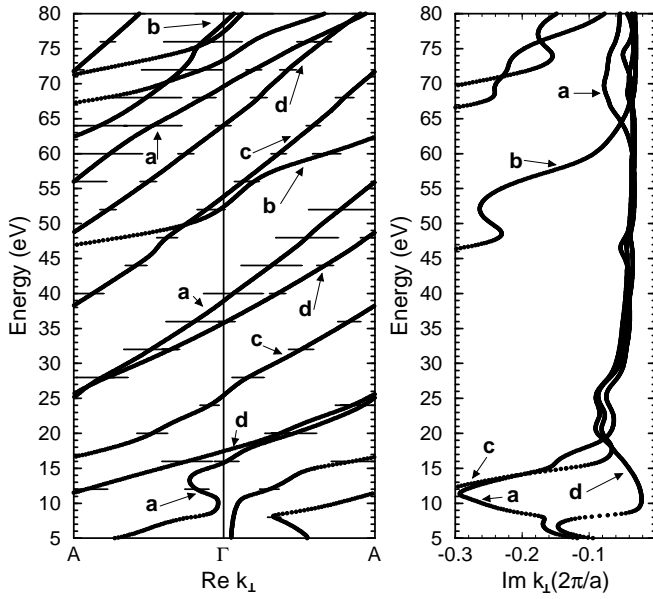


FIG. 5. Complex band structure of GaN for the symmetry line Γ . Bars indicate the magnitude of the expansion coefficients of the valence state with respect to the complex bulk bands.

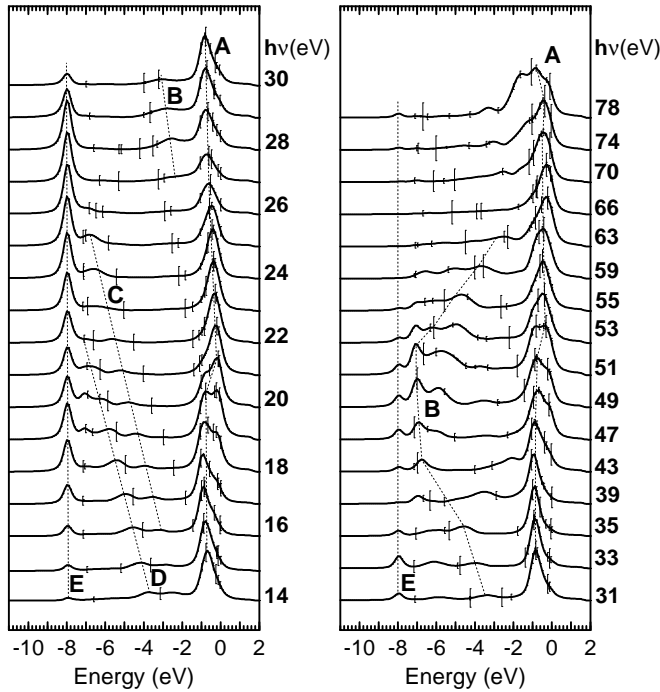


FIG. 6. Theoretical normal emission spectra for GaN (0001)-(1x1)Ga. We have normalized each spectrum separately to an equal amount in the maximum of the photocurrent. The bars indicate binding energies at which direct transitions would be positioned. Their dispersion is drawn by dotted lines as a guide the eye. The energy zero is the VBM, the light is chosen incident along the xz plane with p-polarisation. The spectra are calculated from set A in Table (I).

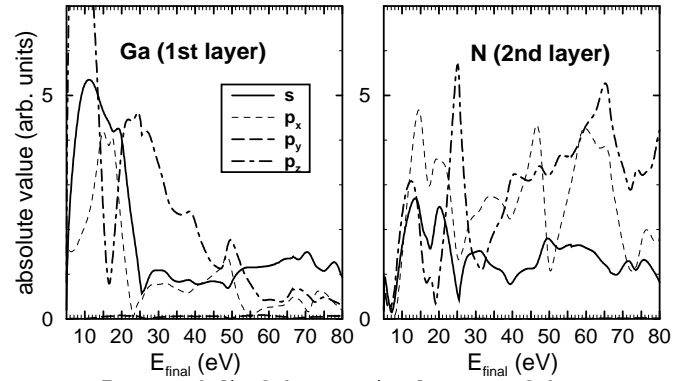


FIG. 7. Moduli of the matrix elements of the two uppermost atomic layers of the GaN (0001)-(1x1)Ga surface resolved into orbitals. The matrix elements are calculated for p-polarized light incident in the xz plane.

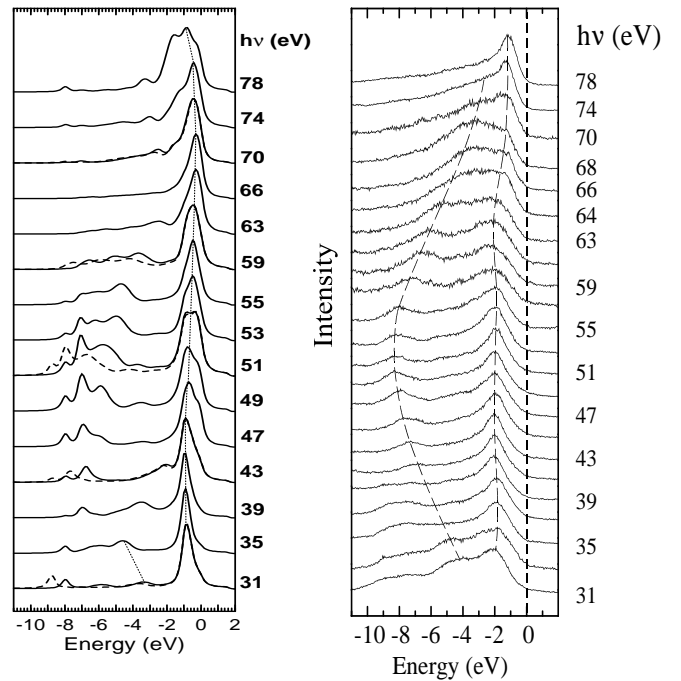


FIG. 8. Comparison between theoretical (left hand side) and experimental photoemission spectra of Desiet al. [8] in normal emission. The theoretical spectra are calculated from set A (see Table I), except for the dashed spectra, which are calculated from set B.

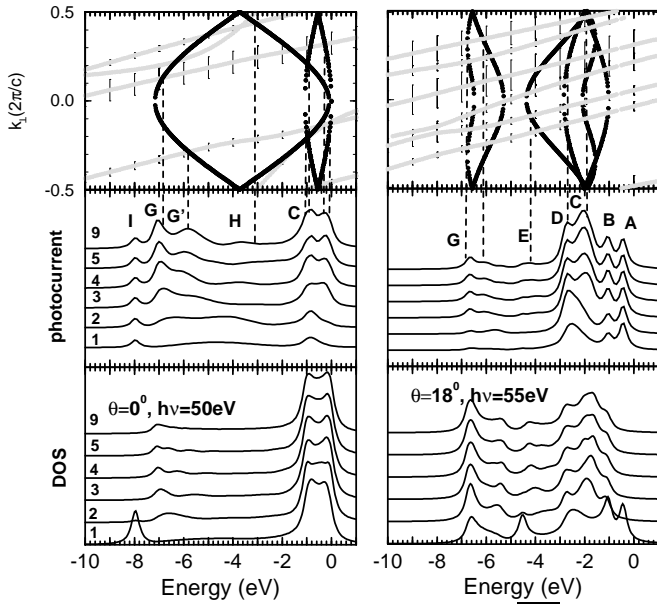


FIG. 9. Layer resolved photocurrent in the M direction for 0 and 18 (middle part) together with the complex bands (grey) and the initial bulk bands (dots) in the top panel. The bands are shifted by the excitation energy and the positions of direct transitions are indicated (vertical dashed lines). The bottom panel shows the layer-resolved density of states. The layer resolved photocurrent is calculated for the number of layers as indicated, each layer consisting of four atomic planes (see text).

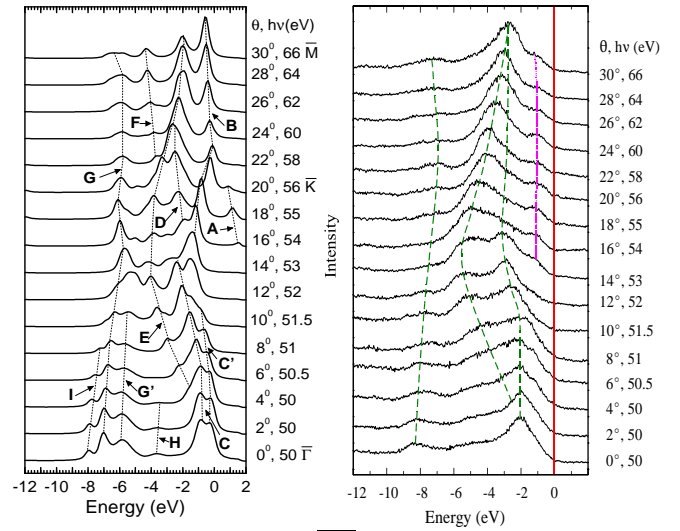


FIG. 11. Results for the K direction. On the left hand side the theoretical photocurrents according to parameter set A, and on the right hand side experimental data from Dhesi et al. [8]

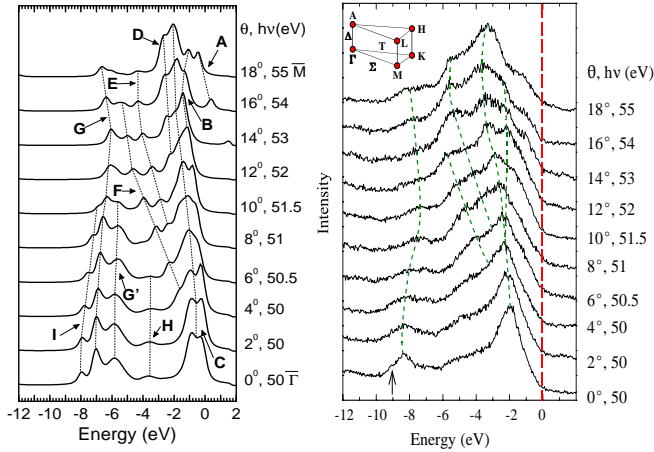


FIG. 10. Results for the M direction. On the left hand side the theoretical photocurrents according to parameter set A, and on the right hand side experimental data from Dhesi et al. [8]. The arrow indicates a weak shoulder to be compared with (I) (see text)

	K_{ss}	K_{sp}	K_{pp}	I_{s0}	I_{p0}	\tilde{I}_{s0}	\tilde{I}_{p0}	I_{s1}	I_{p1}	\tilde{I}_{s1}	\tilde{I}_{p1}
A	1.0	0.90	0.87	49.78	42.00	22.84	12.05	29.53	22.31	16.71	9.61
B	1.0	0.844	0.844	54.66	39.94	20.49	7.76	24.28	21.19	13.82	4.71

TABLE I. EHT parameter for GaN. The first line (set A) is adjusted to the band structure of Vogel et al. [2], while the second line (set B) is adjusted to Rubio et al. [1]. (0 means nitrogen and 1 gallium, for the notation see Starrost et al. [11]).